Speeding up of Sedimentation under Confinement

S. Heitkam,[1,2] Y. Yoshitake,[1,3] F. Toquet,[1] D. Langevin,[1] and A. Salonen[1]

[1]*Laboratoire de Physique des Solides, UMR 8502, Université Paris Sud, 91405 Orsay, France*
[2]*Institut für Strömungsmechanik, Technische Universität Dresden, 01069 Dresden, Germany*
[3]*Nagaoka University of Technology, 1603-1 Kamitomioka, Nagaoka, Niigata 940-2188, Japan*

(Received 3 January 2013; published 24 April 2013)

We show an increase of the sedimentation velocity as small particles are confined in circular capillaries. In general, confinement slows down sedimentation. But, we show that at low Reynolds numbers and in 1D confinement this is not the case. Particle sedimentation velocity is not homogeneous, which can lead to the formation of structures. These structures are enhanced and stabilized in the presence of walls and in the absence of other dissipative mechanisms. As a consequence, it is possible to achieve sedimentation velocities that even exceed the Stokes velocity. The segregation at critical capillary diameters has been directly observed using a large scale model. These simple experiments offer a new insight into the old problem of sedimentation under confinement.

DOI: 10.1103/PhysRevLett.110.178302 PACS numbers: 47.57.ef, 47.55.P−

Sedimentation plays an important role in technical processes like water treatment as well as in natural spectacles like the genesis of river beds. Thus, it has been investigated for more than 200 years [1–3] and is still well studied as many details remain to be clarified [4]. In very dilute systems, the sedimentation velocity u_0 is given by Stokes law, while with increasing particle volume fraction Φ the bulk sedimentation velocity $u_b(\Phi)$ decreases. This decrease is often modeled using the empirical Richardson-Zaki law [5]

$$u_b(\Phi) = u_0(1 - \Phi)^n. \quad (1)$$

The exponent n varies with the particle Reynolds number [6]; for low Reynolds numbers, it is usually between 4.65 and 6.55 [4,7,8].

Sedimentation can take place in strongly confined systems, e.g., in narrow channels or liquid films and plateau borders of foams stabilized by particles or emulsions [9–11]. In these systems, the particle motion is affected by the walls and the sedimentation velocity is observed to decrease with increasing confinement (decreasing D/d, where d is a particle diameter and D the channel width). The walls hinder the movement of the particles by imposing a no-slip boundary condition and slow down the sedimentation. In order to account for this effect, Richardson and Zaki [5] suggest to replace n in Eq. (1) with a new exponent m, which for small Reynolds numbers is written as

$$m = n + 19.5d/D. \quad (2)$$

This describes much of the data rather well, although it does not seem universal [7].

In order to understand the processes better, measurements of the local velocities of individual particles have been performed [8,9,12–14]. Such experiments have shown that during sedimentation the particle velocities are correlated at large scales. Segre *et al.* [9] found that the length of the velocity correlations scales with the interparticle distance $d\Phi^{-1/3}$. The typical size of the correlated regions ranges from 10 to $30d\Phi^{-1/3}$ [9]. However, if the box size limits the size of these structures, the velocity fluctuations become less prominent.

These fluctuations can, but do not necessarily, lead to changes in the particle distribution. The distribution can be expressly changed by different methods, for example, through tilting the tubes, and can have a strong influence on the average sedimentation velocity. Sedimentation velocities in tilted tubes are higher than in vertical ones due to the formation of lanes (akin to large convection cells), a phenomenon known as the Boycott effect [15–17]. A small shear has also been shown to increase the sedimentation velocity [18], which could be linked to the formation of shear bands changing the particle distribution. The formation of particle-rich and particle-poor regions can also occur due to flow instabilities, such as the Rayleigh-Taylor instability, which has been observed even in very dilute systems [19]. The proximity of walls can then influence the particle distribution: Kuusela *et al.* [12] have found that vertical walls can potentially support the formation of concentrated regions of particles. Van Blaaderen and co-workers [20,21] have observed structures similar to those of Rayleigh-Taylor instability in sedimenting suspensions confined between two horizontal plates (the presence of the wall below and above influences the particle distribution and thus the sedimentation). To our knowledge, no one has previously reported the speeding up of sedimentation in cylindrical tubes (1D confinement).

We have investigated the sedimentation of monodisperse polystyrene (PS) particles ($d = 40 \pm 4$ μm, DYNOSEEDS, Microbeads AS) at varying volume fractions ($\Phi = 0.01$–0.5) dispersed in water [Fig. 1(a)]. Complementary to the PS dispersions, we have studied large polymer spheres (BBs, $d = 6$ mm) in glycerol. BBs can be observed with the naked eye, and thus we were able to measure the individual

 © 2013 American Physical Society

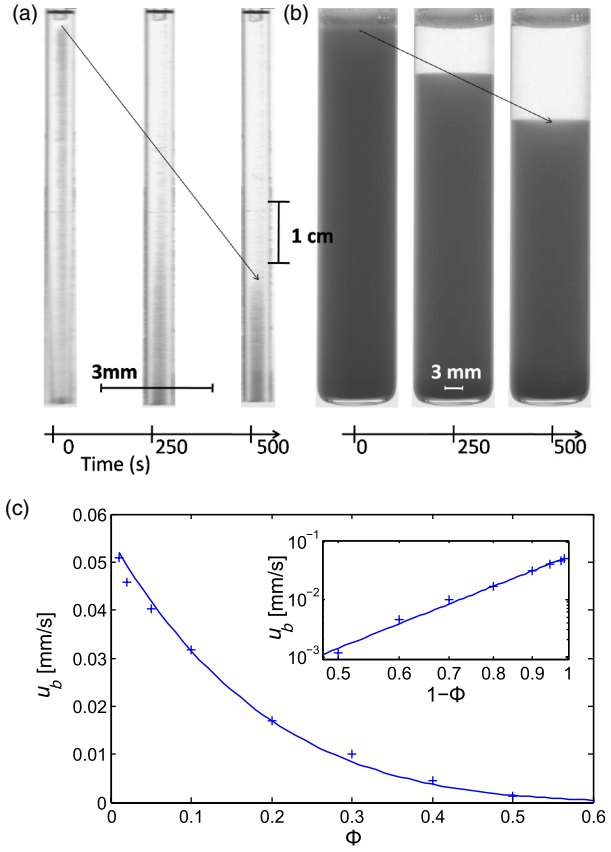

FIG. 1 (color online). Sequence of PS sedimentation ($\Phi = 0.2$) (a) in a small capillary ($D/d = 8.5$) and (b) in a wide capillary ($D/d = 300$), demonstrating the higher sedimentation velocity in the smaller capillary. (c) Bulk sedimentation velocity u_b for different particle concentrations Φ and fit with the Richardson-Zaki law [Eq. (1), $n = 5.25$, $u_0 = 0.055$ mm/s].

particle velocity profiles. The parameters for both dispersions are given in Table I. They were chosen in order to have low Archimedes numbers. Therefore, they are controlled by viscous dissipation and there is no turbulence. The dispersion of the PS particles in water necessitates the addition of 86 mg/L sodium dodecyl sulfate, which does not alter the fluid parameters.

The sedimentation velocities have been measured in round glass capillaries of different inner diameters

TABLE I. Parameters for polystyrene spheres in water (PS) and cellulose spheres in glycerol (BB).

	PS	BB
Particle diameter d	40 μm	6 mm
Fluid kinematic viscosity ν	10^{-6} m^2/s	7.9×10^{-4} m^2/s
Fluid density ρ	998 kg/m^3	1260 kg/m^3
Relative density $\Delta\rho/\rho$	0.05	0.05
Archimedes number Ar	0.032	0.17
Stokes velocity u_0	4.5×10^{-5} m/s	1.3×10^{-3} m/s
Reynolds number Re(u_0, d)	0.002	0.01
Péclet number Pe(u_0, d)	2×10^5	2×10^{14}

($200 \leq D \leq 1470$ μm and 1.2 cm). The capillary is filled [22] and mounted on a vertical holder (angle from vertical ± 0.3 degree) and is closed at the top to prevent evaporation. As the sedimentation progresses, the particles move downward, leaving behind clear water separated by a sharp frontier, as is demonstrated in Figs. 1(a) and 1(b). The velocity of the sedimentation frontier u_s was determined by taking sequences of images in transmission with a CCD camera. The brightness distribution variation with height was determined by subtracting the background and averaging brightness horizontally. Because the frontier between water and the sedimenting dispersion is somewhat diffuse, we used two thresholds with a high and a low brightness limit, respectively, giving two positions along the capillary. Their time variation was fitted with a linear function, which led to an upper and a lower limit for the sedimentation velocity. The image treatment is described in more detail in the Supplemental Material [23].

In Fig. 1(c), the bulk sedimentation velocities measured at large D ($D = 1.2$ cm) of PS particles are compared to the Richardson-Zaki law [Eq. (1)]. The measurements can be fitted with the equation using $n = 5.25$ and $u_0 = 0.055$ mm/s. The value of u_0 is close to the theoretical value, given in Table I, while n is in good agreement with Ref. [5]. This confirms the absence of particle aggregation in the dispersion.

Turning our attention to sedimentation in the capillaries, the difference in the sedimentation velocities is clear in the two series of photos in Figs. 1(a) and 1(b). The sedimentation velocity u_s (a) in the thin capillary is much higher than (b) in the bulk. This finding completely conflicts with the prediction, made by Eq. (2), that confinement slows down the sedimentation. We have measured systematically the influence of capillary diameter D/d and particle concentration Φ on the sedimentation velocity u_s, reported in Fig. 2(a). A maximum of u_s is observed for medium size capillaries for all Φ, most prominent for $\Phi = 0.1$. The maximum moves to lower D/d with increasing Φ. In order to compare the different data sets, the sedimentation velocity u_s is normalized with the bulk sedimentation velocity u_b. However, as we are working with small capillaries, the expected sedimentation velocity changes and should be corrected for, as proposed by Richardson and Zaki [Eq. (2)]. In order to avoid using the empirical relation (2), we take into account the excluded volume near the walls (the particle centers have to be situated within a reduced tube diameter $D - d$ because they cannot penetrate the wall). This leads to an effective volume fraction Φ_{eff} higher than in the bulk, as given in Eq. (3),

$$\Phi_{\text{eff}} = \Phi/(1 - d/D)^2. \quad (3)$$

The fraction of excluded volume becomes more important as D decreases, and the difference between Φ and Φ_{eff} is larger as Φ increases. Inserting the effective volume fraction into the first Richardson-Zaki relation [Eq. (1)] but keeping n constant yields a corrected bulk velocity

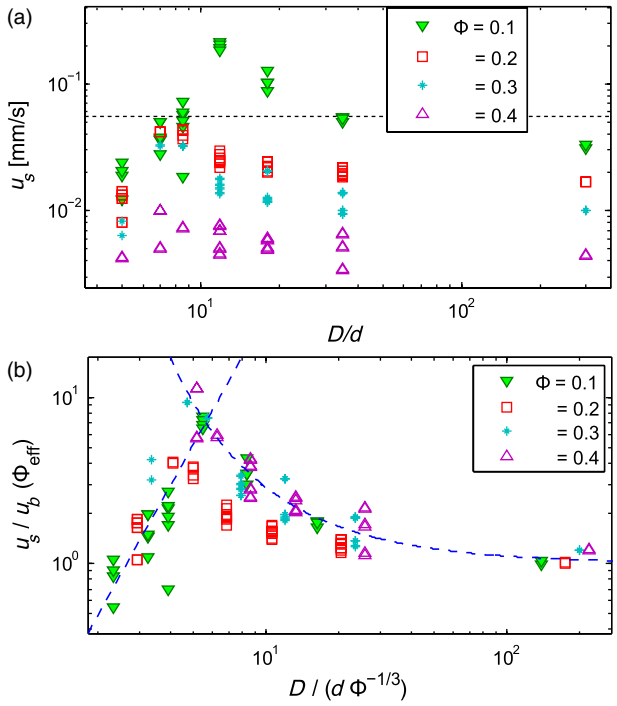

FIG. 2 (color online). Downward velocity u_s of the sedimentation frontier for different PS particle concentrations Φ and relative capillary diameters D/d (a) unnormalized and (b) normalized with interparticle distance $d\Phi^{-1/3}$ and bulk sedimentation velocities $u_b(\Phi_{\text{eff}})$ at the referring effective particle concentration Φ_{eff}, given by Eqs. (3) and (4). Dashed lines (a) mark u_0 or (b) serve as guides to the eye.

$$u_b(\Phi_{\text{eff}}) = u_0(1 - \Phi_{\text{eff}})^n. \tag{4}$$

The velocity $u_b(\Phi_{\text{eff}})$ was used in Fig. 2(b) to normalize the sedimentation velocity u_s. It is interesting to note that the expression $u_b(\Phi, D/d)$, given by Eqs. (3) and (4), leads to similar u_b values as in Eqs. (1) and (2), as demonstrated in the Supplemental Material [24]. This shows that the empirical dependence of m can be properly described by an excluded volume effect.

The position of the maximum also depends on Φ. Following Segre *et al.* [9], we normalize D with the interparticle distance $d\Phi^{-1/3}$ implying the role of how much the particles can be compacted. With this renormalization of u_s and D, the data fall onto a master curve in Fig. 2(b). The unusual maximum in the sedimentation velocity at normalized diameters of approximately $D/(d\Phi^{-1/3}) \approx 5$ to 20 is clearly visible. Segre *et al.* [9] found normalized velocity correlation lengths s of roughly $s/(d\Phi^{-1/3}) \approx 10$ to 30 which are comparable to the capillary diameters at which the speed up of sedimentation appears. We therefore propose that the speeding up takes place because of the wall-supported stabilization of these fluctuations in the sedimentation process, leading to the formation of particle-rich and particle-poor regions which sediment in separate lanes.

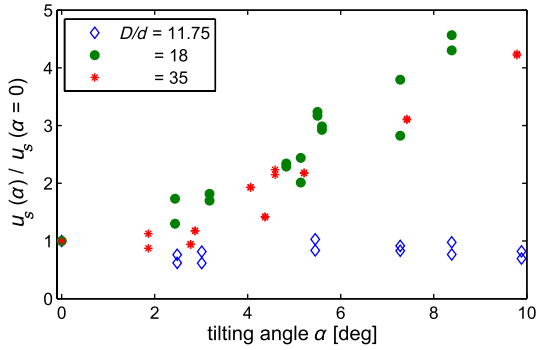

FIG. 3 (color online). Sedimentation velocity u_s for $\Phi = 0.1$ PS at different capillary diameters and tilt angles α, normalized with the corresponding vertical sedimentation velocity at $\alpha = 0$.

This remarkable feature appears exclusively under certain conditions. The Archimedes number, and thus the particle Reynolds number, has to be very low. In our experiments, the Reynolds number was below 0.01, so turbulence is absent. The sedimentation of BB particles in water ($\Phi = 0.1$, $D/d = 10$) with a Reynolds number of 4000 is in agreement with Eq. (1), well below the Stokes velocity. Speeding up did not occur. The geometry of confinement also plays an important role. We have investigated the sedimentation of PS spheres ($\Phi = 0.1$) between two vertical plates of $10d$ distance (2D confinement). The resulting sedimentation velocity is 0.028 mm/s, slightly smaller than the bulk sedimentation velocity of 0.03 mm/s. This shows the importance of circular confinement.

The formation of stable concentration gradients is similar to the Boycott effect, where they are induced and stabilized by a small vertical tilt. This leads to an increase in the sedimentation velocity as well. In order to observe how the intentional formation of lanes influences sedimentation, we carried out experiments tilting our capillaries. The tilt angle α is measured with a plumb line. The influence of small tilt angles on the drainage velocity at $\Phi = 0.1$ and three different capillary diameters is reported in Fig. 3. Figure 3 shows that tilting increases the sedimentation velocity for the large capillaries. The accumulation of particles at the wall, and thus the sedimentation velocity, is increased with increasing tilt angle as expected. However, for $D/d = 11.75$, almost no influence of the angle was found. This supports our explanation above: In the smaller capillary particle accumulation at the wall occurs even without tilting, and tilting does not enhance it. Figure 3 also demonstrates that small uncertainties in verticality have only a small impact on the measured sedimentation velocity. However, in the experiments of Fig. 2, the verticality was well controlled and we can exclude any influence of the tilt angle on these data.

To further support our interpretation, we observed directly the flow of individual particles during the sedimentation. To do so, we used the cellulose spheres (BB, Table I), a large scale model of the sedimentation in

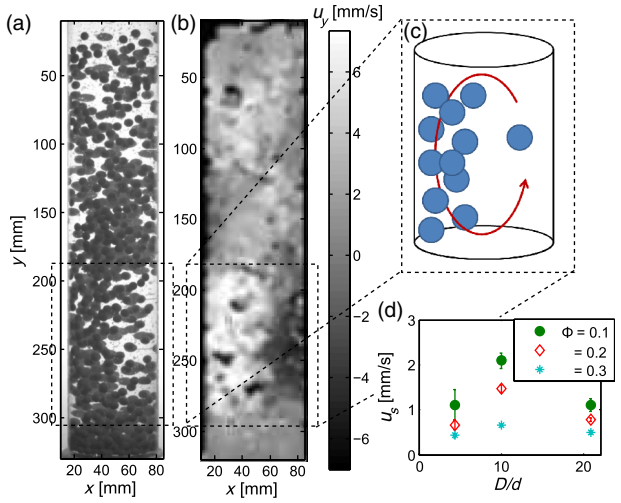

FIG. 4 (color online). (a) Snapshot of BB sedimentation, (b) its corresponding sedimentation velocity distribution, (c) sketch of the diffusion cell, and (d) sedimentation front velocity for different concentrations and relative diameters.

capillaries. Figure 4(a) shows a snapshot of the sedimentation of BBs in a medium diameter tube ($D/d = 10$). By correlating two consecutive images, we determine the average local velocity of the BBs, presented in Fig. 4(b). In the highlighted area, particles accumulate at the left wall of the tube. Thus, they sediment very fast. The right side is particle poor, and the few particles in this region move upward, as is sketched in Fig. 4(c). This convection structure results in a speeding up of sedimentation in the BB system as well, as is reported in Fig. 4(d). This demonstrates that the speeding up is purely a feature of fluid mechanics, hardly dependent on the physical chemistry of the particle surface.

In conclusion, we have reported an increase in sedimentation velocity in capillaries that can even exceed Stokes velocity. The initially homogeneous sedimentation is an unstable state: Spontaneously, or by interaction with the wall [25], small disturbances in the particle distributions can appear, resulting in an imbalance of the gravitational force. Regions with a higher particle fraction move downward faster and collect more and more particles while the clear liquid avoids particle-rich regions and flows upward in particle-poor regions. So, the imbalance is amplified, resulting in the formation of structures inside the sedimentation process. These structures have been investigated experimentally [8,9,13] and numerically [14]. Typical structure sizes, measured by spatial correlation, equal about 10 to $30d\Phi^{-1/3}$ [8,9,13,14,26]. In our experiments, the speed up of sedimentation is most prominent in capillaries of diameters similar to that value (5 to $20d\Phi^{-1/3}$). As demonstrated in an up-scaled experiment, the convection structure is stabilized and fills the whole cross section of these capillaries, enhancing the sedimentation significantly. To the best of our knowledge, this feature has not been reported before. The reason for that might be that it is very sensitive to the Archimedes number and thus to the particle Reynolds number. In our PS system, with a Reynolds number of 0.002, a sedimentation velocity of up to 4 times the Stokes velocity or 6 times the bulk sedimentation velocity $u_b(\Phi)$ was measured. In the BB system ($\mathrm{Re} = 0.02$), the maximum velocity was only $2 \times u_b(\Phi)$. Note that in the experiments of DiFelice and Parodi [7], who studied a similar system with $\mathrm{Re} = 0.15$, the maximum sedimentation velocity was only $1.05 \times u_b(\Phi)$, and this increase was not discussed by the authors, possibly because it was within experimental uncertainty. Therefore, the speed up seems to be present only at very low Reynolds numbers. Higher Reynolds numbers lead to unordered particle movement and thus disintegrate the sedimentation structures. Additionally, if the particles are too small, Brownian motion may tend to equalize the particle distribution and thus possibly disintegrate the sedimentation structures. Finally, the speeding up depends on the geometry of the confinement. In a circular capillary of $10d$ diameter, the sedimentation is faster, while, between two parallel vertical plates separated by the same distance, no speeding up is observed. We assume that the reason for this is the difference in the shape of the velocity gradients of the continuous fluid. Particle concentrations can be altered by velocity gradients, according to the Basset-Boussinesq-Oseen equation [27], but the complex interactions between particles and the continuous fluid will make the complete theoretical description of the problem difficult. The acceleration of sedimentation could be of importance for particles and emulsion droplets in microfluidic devices or in foam Plateau borders, when stable convection cells could also be present. By adding ascending particles to the sedimentation process, it is even possible to enforce the formation of convection cells in the absence of walls [28].

We acknowledge Véronique Trappe, Phil Segrè, Jochen Fröhlich, Elisabeth Guazzelli, and Florence Rouyer for fruitful discussions. This work was partially financed by the French Ministry of Foreign and European Affairs.

[1] K. Scott, J. Ritter, and J. Knott, U.S. Geol. Surv. Water-Supply Pap. E1 (1798).
[2] J. Raymond, Public Heal. Pap. Rep. **16**, 132 (1890).
[3] F. Fitzpatrick, J. Knox, and J. Schubauer-Berigan, Upper Mississippi River National Wildlife and Fish Refuge, Wisconsin, 1846-2006.
[4] R. Blazejewski, Int. J. Multiphase Flow **39**, 179 (2012).
[5] J. Richardson and W. Zaki, Chem. Eng. Sci. **3**, 65 (1954).
[6] P. Snabre and P. Mills, Eur. Phys. J. E **1**, 105 (2000).
[7] R. Di Felice and E. Parodi, Am. Inst. Chem. Eng. **42**, 927 (1996).
[8] H. Nicolai, B. Herzhaft, E. J. Hinch, L. Oger, and E. Guazzelli, Phys. Fluids **7**, 12 (1995).
[9] P. N. Segre, E. Herbolzheimer, and P. M. Chaikin, Phys. Rev. Lett. **79**, 2574 (1997).

[10] S. Y. Tee, P. J. Mucha, L. Cipelletti, S. Manley, M. P. Brenner, P. N. Segre, and D. A. Weitz, Phys. Rev. Lett. **89**, 054501 (2002).
[11] F. Rouyer, C. Fritz, and O. Pitois, Soft Matter **6**, 3863 (2010).
[12] E. Kuusela, J. M. Lahtinen, and T. Ala-Nissila, Phys. Rev. E **69**, 066310 (2004).
[13] P. N. Segre, F. Liu, P. Umbanhowar, and D. A. Weitz, Nature (London) **409**, 594 (2001).
[14] M. P. Brenner, Phys. Fluids **11**, 754 (1999).
[15] T. Séon, Ph.D. thesis, Universite Pierre and Marie Curie, 2006.
[16] T. Seon, J. Znaien, B. Perrin, E. J. Hinch, D. Salin, and J. P. Hulin, Phys. Fluids **19**, 125105 (2007).
[17] M. Debacq, J. P. Hulin, D. Salin, B. Perrin, and E. J. Hinch, Phys. Fluids **15**, 3846 (2003).
[18] K. Benes, P. Tong, and B. J. Ackerson, Phys. Rev. E **76**, 056302 (2007).
[19] D. Velegol, S. Shori, and C. E. Snyder, Ind. Eng. Chem. Res. **48**, 2414 (2009).
[20] C. P. Royall, J. Dzubiella, M. Schmidt, and A. van Blaaderen, Phys. Rev. Lett. **98**, 188304 (2007).
[21] A. Wysocki, C. P. Royall, R. G. Winkler, G. Gompper, H. Tanaka, A. van Blaaderen, and H. Lowen, Soft Matter **5**, 1340 (2009).
[22] See Supplemental Material at http://link.aps.org/supplemental/10.1103/PhysRevLett.110.178302 for detailed description of the filling process.
[23] See Supplemental Material at http://link.aps.org/supplemental/10.1103/PhysRevLett.110.178302 for detailed description of the image processing.
[24] See Supplemental Material at http://link.aps.org/supplemental/10.1103/PhysRevLett.110.178302 for a detailed description of the normalization.
[25] D. Bruneau and F. Feuillebois, Phys. Fluids **8**, 2236 (1996).
[26] E. Guazzelli and J. Hinch, Annu. Rev. Fluid Mech. **43**, 97 (2011).
[27] E. Loth, Prog. Energy Combust. Sci. **26**, 161 (2000).
[28] R. L. Whitmore, Br. J. Appl. Phys. **6**, 239 (1955).